Gas emission optimization and optimal energy management of a microgrid operating by renewable and sustainable generation systems

Nabil MEZHOUD[(1)*], Bilel AYACHI[(1)], Ahmed BAHRI[(2)]
[(1)] Electrical Engineering Department, LES Laboratory, Faculty of Technology, University 20 Août 11955-Skikda, Algeria.
[(2)] Department of Automatics and Electromechanics, Faculty of science and technology, Materials, Energy Systems Technology and Environment Laboratory, Ghardaïa University, Ghardaïa, 47000, Algeria.
[*]Corresponding author: n.mezhoud@univ-skikda.dz

Abstract: The economic operation of electric energy generating systems is one of predominant problems in energy systems. Due to the need for better reliability, high energy quality, lower losses, lower cost and clean environment, the application of renewable and sustainable energy sources such as wind energy, solar energy, fuel cells, etc. in recent years has become more widespread mainly. In this work, one of most general of all swarm intelligence algorithms inspired by collective intelligent behavior of natural or artificial systems called the Particle Swarm Optimization (PSO) is applied to solve the Gas emission Optimization (GEO) and the Optimal Energy Management (OEM) problems of a micro-grid (MG) operating by Renewable and Sustainable Generation Systems (RSGS). Our main goal is to minimize nonlinear objective function of an electrical micro-grid taking into account of equality and inequality constraints. The PSO approach was examined and tested on a standard MG system composed of different types of RSGS such as wind turbines (WT), photovoltaic systems (PV), fuel cells (FC), micro turbine (MT), diesel generator (DEG) and loads with energy storage systems (ESS). The results are promising and show the effectiveness and robustness of proposed approach to solve the GEO and the OEM problems. The results of proposed method have been compared and validated with those known references published recently.

Keywords: Renewable energy sources, energy management, distributed generator, micro-grids, particle swarm optimization

1. INTRODUCTION

The introduction section must contain theory related to the paper topic along with state of art study and well referenced citations. Make this section as informative as possible to justify the work and situate it with respect to the literature.

The development and exploitation of renewable energies have experienced strong growth in recent years [1]. Among these sources of energy, wind generators occupy a special place. In fact, on the one hand, wind energy is expected to develop strongly in many regions, and on the other hand, this very fluctuating energy, due to significant variations in wind speed, can significantly affect the quality of the voltage and current in the network where it is injected [2].

Electric power plants that operate on Esoteric-fuel are among the most prominent sources of air pollution and contribute to causing great harm to the environment due to the burning of raw fuels such as coal, gas, and oil [5]. The burning of coal contributes a large proportion of polluting gases to the Earth's atmosphere, as it produce large amounts of Carbon oxides CO_2, and some toxic and dangerous gases such as emissions of Sulfur oxides SO_x, and Nitrogen oxides, NO_x. The quantity and nature of the pollutant depends on the type and quality of the used fuel [4]-[5].

The emission index, or environmental index, is considered an important indicator from a conservation point of view [3]. Several strategies have been proposed and discussed to reduce atmospheric emissions.

After implementation of the 1990 amendment to the United States Clean Air Act and increasing public awareness of environmental protection and public utilities, electricity production companies were obligatory to adapt their designs and making strategies to reduce pollution rate and emissions of electric power plants [3]-[4].

Over the past two decades, distributed generation (DG) has experienced steady growth. The integration of DGs with renewable energies sources (RES) such as photovoltaic systems (PV) and small wind turbines (WTs) depends on geographical and meteorological conditions. Furthermore, the natures of their output powers both vary over time and are difficult to predict. On the other hand, non-renewable energy DG units, such

as fuel cells (FC), micro turbines (MT), diesel generators (DEG), and energy storage systems can be connected to any point of the distribution network and have predictable output power [6-7].

In general, DG units, if well planned and controlled, can improve power quality, reduce power losses, improve reliability and reduce emissions. A good way to realize the maximum potential of DG is to coordinate operation and control with storage devices and controllable loads. This leads to the concept of micro-grids (MGs) [8-9]. Therefore, a MG can be defined as a local distribution network comprising various DG units, controllable loads and energy storage systems, which can operate either interconnected or isolated from the main distribution network.

MGs represent the core of intelligent distribution networks within modern power systems. In order to take full advantage of the operation of MGs, such as improved profitability and reduced dependence on the main network, it is important that the integration of DGs into MGs, and their relationship with the distribution network main upstream, helps to optimize the general operation of the system. To achieve this goal, it is necessary to use the appropriate control system architecture [10]-[13].

Energy management is one closely related concept that aims to optimize usage in a given system. Energy management refers to the overall management of energy within a system, seeking to minimize losses and maximize energy efficiency. This is a nonlinear optimization problem with constraints named optimal Energy and Operation Management (EOM) [14].

In recent years, many population-based optimization techniques have been used to solve complex constrained optimization problems such as linear programming algorithm [15], genetic algorithm (GA) [7], [16], The non dominated sorting GAII [17], particle swarm optimization (PSO) [5], [14], modified particle swarm optimization (MPSO) [18], mesh adaptive direct search [19], gravitational search algorithm (GSA) [20], firefly algorithm (FFA) [21], modified firefly algorithm (MFFA) [22], artificial bee colony (ABC) [23], Bacterial foraging algorithms (BFA) [24], cuckoo search algorithm (CSA) [25], harmony search [26], evolution programming (EP) [27], differential evaluation (DE) [28], moth Swarm Algorithm (MSA) [29], wind driven optimization method (WDO) [30], teaching-learning-studying-based optimization (TLBO) [31], sine-cosine algorithm (SCA) [32], modified imperialist competitive algorithm (MICA) [33], electromagnetism-like mechanism method (ELM) [34], ant colony optimization (ACO) [35], shuffled Frog leaping algorithm (SFLA) [36], and more recently grey wolf optimizer (GWO) [4], [37]-[38]. In this work, the PSO approach is used to solve the GEO and OEM problems.

2. PROBLEM FORMULATION

Generally, the GEO and OEM problems can be expressed as follows [39].

$$Min\ f(x,\ u) \quad (1)$$

Subject to

$$h(x,\ u) = 0 \quad (2)$$

$$g(x,\ u) \le 0 \quad (3)$$

$$x_{\min} \le x \le x_{\max} \text{ and } u_{\min} \le u \le u_{\max} \quad (4)$$

$f(x,u)$ is the objective function. $h(x,u)$ and $g(x,u)$ are, respectively, the equality and inequality constraints. x and u are the state and control variables respectively.

2.1. Objective function

2.1.1 Gas emission optimization

Generally, the GEO problem can be expressed as follows

$$\min\ f(x,u) = \min \sum_{k=1}^{n_g} 10^{-2}\left(\alpha_k + \beta_k P_{gk} + \gamma_k P_{gk}^2\right) + \zeta_k \exp\left(\lambda_k P_{gk}\right) \quad (5)$$

Hence, x and u can be expressed as given

$$x^t = \left\{P_{G_1}, |V_{L_1}|, ... |V_{L_{nL}}|, Q_{G_1}, ... Q_{G_{ng}}, S_1, ..., S_{n_{br}}\right\} \quad (6)$$

Where, P_G, Q_G, V_L and S_k are the generating active power at slack bus, reactive power generated by all generators, magnitude voltage of all load buses and apparent power flow in all branches, respectively. n_g, n_L and n_{br} are, respectively, the number total of generators, the number total of load buses and the number total of branches. The set control parameters are represented in terms of the decision vector as follows [39]-[40]:

$$u^t = \left\{P_{g_2}, ..., P_{g_{ng}}, |V_{g_1}|, ... |V_{g_{ng}}|, Q_{1_{com}}, ... Q_{n_{com}}, T_1, ..., T_{n_T}\right\} \quad (7)$$

Where, P_G are the active power generation excluding the slack generator, V_G are the generators magnitudes voltages T is tap settings transformers, and Q_{com} are the reactive power compensation by shunt compensators, n_{com} and n_T are the number total of compensators and the number total of transformers, respectively.

$$\begin{cases} P_{gk} = P_k + P_{dk} \\ Q_{gk} - Q_{comk} = Q_k + Q_{dk} \end{cases} \quad (8)$$

Where P_{gk} and Q_{gk} are the scheduled active and reactive power generations at bus k, respectively. P_k, Q_k are the active and reactive power injections at bus *k*. P_{dk}, Q_{dk} and Q_{comk} are the active and reactive power loads and the reactive power compensation at bus k. The inequality constraints $g(x,u)$ are represented by the system operational and security limits, listed below [40].

$$P_{gk}^{\min} \le P_{gk} \le P_{gk}^{\max} \quad \text{where } k = 1,.....,n_g \quad (9)$$

$$Q_{gk}^{\min} \le Q_{gk} \le Q_{gk}^{\max} \text{ where } k = 1,.....,n_g \quad (10)$$

$$V_k^{\min} \le V_k \le V_k^{\max} \quad \text{where } k = 1,.....,n_b \quad (11)$$

$$\theta_k^{\min} \le \theta_k \le \theta_k^{\max} \quad \text{where } k = 1,.....,n_b \quad (12)$$

$$T_k^{\min} \le T_k \le T_k^{\max} \quad \text{where } k = 1,.....,n_T \quad (13)$$

$$Q_{Comk}^{\min} \le Q_{Comk} \le Q_{comk}^{\max} \text{ where } k = 1,.....,n_{Com} \quad (14)$$

$$S_{kj} \le S_{kj}^{\max} \quad \text{where } k = j = 1,.....,n_b \quad (15)$$

Where, T , Q_{Com} n_T , n_{Com} and $S_{kj}^{\max}$ are the transformers tap settings, the reactive power compensation, the number total of transformers, the number total of compensator and the maximum apparent power between buses k and j.

2.1.2. Optimal energy management

OEM is nonlinear and non-convex optimization problems with constraints, the main objective is to minimize the operating costs of the MG. In general, the OEM can be presented as follows [41]:

$$\min f(x,u) = \sum_{t=1}^{NT} \cos t^t \left(x^t, u^t\right) = \min_u \sum_{t=1}^{NT} \sum_{i=1}^{NG} \left[B_{Gi}\left(P_{Gi}^t\right) + MP^t P_{Grid}^t\right] \quad (16)$$

$f(x,u)$ represent the overall operating cost of the MG systems over the planning horizon; *T* is a scalar objective function. The decision variables can be the powers of the DG, the battery, the demand response (DR) and shedding. In this case, the state variables vector x^t that is bought (sold) from to the utility is:

$$x^t = P_{Grid}^t \quad (17)$$

The control variables vector u^t including the active power of the generation and storage units inside the MG can be expressed as follows:

$$u^t = \left[P_{Gi}^t,\ P_{G2}^t,....P_{GNG}^t\right] \quad (18)$$

Where, NT is the total number of time (hours) in the considered period, NG is the total number of DGs including storage units, P_{Gi}^t is the output active power of the *i*th DG at time *t*, $B_{Gi}(P_{Gi}^t)$ is the bid of the *i*th DG based on its active power at time *t*, P_{Grid}^t is the active power that is bought (sold) from (to) the utility at time t, and MP^t is the market price of the exchange of electricity between the MG and the utility at time *t*. Generally, the cost function (16) is a non-linear function because the offers of DG are, generally, a piecewise linear or quadratic function of P_{Gt} [42].

$$u^t = \left[P_{Gi}^t,\ P_{G2}^t,....P_{GNG}^t\right] \quad (19)$$

2.2. Constraints

1 Power balance constraints (PBC)

For each time interval t, the total power output of DGs, energy storage devices and utility must cover the total demanded load in the MG. As a result of MG with power loss is neglected, the power balance constraint can be represented as follows:

$$\sum_{i=1}^{NG} P_{Gi}^t + P_{Grid}^t = \sum_{D=1}^{ND} P_{L_D}^t \quad (20)$$

P_{L_D} is the quantity of the Tenth loads level and ND is the total number of loads levels.

2 Power generation capacity constraints

For stable operation, the active power output of each unit in the MG, including the utility, is limited by the maximum and minimum limits as follows:

$$P_{Gi,\min}^{t} \le P_{Gi}^{t} \le P_{Gi,\max}^{t} \quad (21)$$

$$P_{Grid,\min}^{t} \le P_{Grid}^{t} \le P_{Grid,\max}^{t} \quad (22)$$

$P_{Gi,\min}^{t}$, $P_{Grid,\min}^{t}$, $P_{Gi,\max}^{t}$ and $P_{Grid,\max}^{t}$ are the minimum and maximum active powers of the i^{th} DG, and the utility at time t, respectively.

3 Reserve spinning constraints (RSC)

The RSC is necessary to maintain the reliability of the system, due to the power fluctuations of the renewable and the load fluctuations. To satisfy the RS, the following inequality constraint must be satisfied [43]:

$$\sum_{i=1}^{NG} P_{Gi,\max}^{t} + P_{Grid,\max}^{t} = \sum_{D=1}^{ND} P_{L_D}^{t} + R^{t} \quad (23)$$

R^t is the spinning reserve programmed at time t. In an MG, the spinning reserve constraint is considered by adding an additional value to the total power demand, which should be supplied by the DG units. It should be noted that the maximum power (not the operating point) of the energy sources is considered in the above equation.

4 Energy storage limits (ESL)

Since there are certain limits to the charge and discharge rate of storage devices during each time interval, the following equation and constraints can be expressed [44]:

$$W_{ess,t} = W_{ess,t-1} + \eta_{charge} P_{charge} \Delta t - \frac{1}{\eta_{discharge}} P_{discharge} \Delta t \quad (24)$$

$$\begin{cases} W_{ess,\min} \le W_{ess,t} \le W_{ess,\max} \\ P_{charge,t} \le P_{charge,\max} \quad and \quad P_{discharge,t} \le P_{discharge,\max} \end{cases}$$

$W_{ess,t}$ and $W_{ess,t-1}$ are the amount of energy stored in the battery at time *t* and *t-1*, respectively; $P_{charge}(P_{dechcharge})$ is the charge (discharge) rate allowed for a defined period of time Δt; $\eta_{charge}(\eta_{dechcharge})$ is the efficiency (yield) of the battery during the charging (discharging) process; $W_{ess,\min}$ and $W_{ess,\max}$ are the lower and upper limits of the amount of energy stored inside the battery; and $P_{charge,\max}(P_{dischargee,\max})$ is the maximum rate of charge (discharge) of the battery during each interval time Δt.

5 Calculation of active power from (to) the grid

To apply the active power budget constraint given in (20), the active power from (to) the utility is considered as a dependent variable. The grid power is calculated using the following equation:

$$P_{Grid}^{t} = \sum_{D=1}^{ND} P_{L_D}^{t} - \sum_{i=1}^{NG} P_{Gi}^{t} \quad (25)$$

P_{Gi}^{t} we check whether or not satisfies the constraint defined in (22). Therefore, the variable $P_{Grid,\lim}^{t}$ is defined as:

$$P_{Grid,\lim}^{t} = \begin{cases} P_{Grid,\max}^{t} & si \ P_{Grid}^{t} > P_{Grid,\max}^{t} \\ P_{Grid,\lim}^{t} & si \ P_{Grid,\lim}^{t} < P_{Grid,\min}^{t} \\ P_{Grid}^{t} & si \ P_{Grid,\min\, m}^{t} \le P_{Grid,\min}^{t} \le P_{Grid,\max}^{t} \end{cases} \quad (26)$$

It should be mentioned that the control variables are self-controlled while the dependent variable, i.e. P_{Gi}^{t}, should be added to the objective function as a quadratic penalty term. In this term, a penalty factor multiplied by the square of the difference between the actual value and the limit value of the dependent variable is added to the objective function. The new extended objective function to be minimized is:

$$\min_{u} F_p = \min_{u} \sum_{t=1}^{NT} \cos t^{t}\left(x^{t}, u^{t}\right) + \lambda_p \left(P_{Grid}^{t} - P_{Grid,\lim}^{t}\right)^2 \quad (27)$$

Where λ_p is the penalty factor.

2.3. Bids calculation of distributed generation

The DG bids are considered quadratic, as shown in (28).

$$B_{Gi} = a_i P_{Gi}^{\ 2} + b_i P_{GI} + c_i \quad (28)$$

1 Micro-turbine and Fuel cell

The MT and FC bids in ($/h) can be calculated as follows [19], [45]:

$$B_G = C_{fuel} \frac{P_G}{\eta_G} + C_{inv} \quad (29)$$

Where, P_G is the electrical output power (kW) of the DG, η_G is the electrical efficiency of the DG, C_{fuel} is the price of fuel (natural gas) to supply the DG ($/kWh), C_{inv} is the hourly amount of reimbursement of the investment cost of DG in ($/h). C_{inv} is a

function of the annual investment cost (AC) in ($/kW-year), the annual production (AP) in (kWh/kW) and the nominal power of the DG in (kW):

$$C_{inv} = AC\frac{P_{G,nom}}{AP} \quad (30)$$

$$AC = \frac{i(1+i)^n}{(1+i)^n - 1} IC \quad (31)$$

i is the interest rate, *n* is the amortization period in years, and IC is the installation cost of the DG [46]. The MT electrical efficiency characteristic can be estimated as a quadratic function of its output power. These coefficients can be obtained by fitting the electrical efficiency curve of the MT based on the manufacturers' data. The FC efficiency is a non-linear function of the power level and can be expressed as follows (for a proton exchange membrane fuel cell: PEM-FC) [47]:

$$\eta_{FC} = \frac{1}{2.964}\left[V_0 + \sqrt{V_0^2 - 4\left(V_0 V_{Pnom} - V_{Pnom}^2\right)\xi}\right] \quad (32)$$

V_0 is the theoretical or thermodynamic FC potential (0.9 V), is the potential of the selected cell at rated power (0.45–0.75 V), $\xi = P_{FC}/P_{nom}$ is the power level, and P_{nom} is the rated FC power. The coefficients of the quadratic function (28) can be obtained by curve fitting, constructed according to (29) for a power range of PG.

2 Wind turbines and Photovoltaic

The bid functions of WT and PV consider the annual investment cost for depreciation of equipment (AC) ($/kW) and the annual energy production per kW (AP) (kW h/kW):

$$B_G = C_{fuel}\frac{P_G}{\eta_G} + C_{inv} \quad (33)$$

Where AC is defined by (31), IC is the installation cost of the DGs, (WT and PV). DGs based on renewable sources, for example, WT and PV productions are determined by the availability of the primary source, i.e. Wind or Solar irradiation. According to [48]-[49], the power curve of a WT can be modeled by means of a function divided into four different parts:

$$P_{WT} = \begin{cases} 0 & v \le v_{ci} \\ \dfrac{v^2 - v_{ci}^2}{v_{nom}^2 - v_{ci}^2} P_{WT,nom} & v_{ci} < v \le v_{nom} \\ P_{nom}, & v_{nom} < v \le v_{co} \\ 0 & v \ge v_{co} \end{cases} \quad (34)$$

Where, $P_{WT,nom}$, v_{nom}, v_{ci} and v_{co} are, respectively, the rated power, rated wind speed, switch-on wind speed and switch-off wind speed of the WT; P_{WT} is denote the output power of the WT and v is the wind speed [49].

The PV output power depends on the solar irradiation and the ambient temperature of the site as well as the characteristics of the module itself. To calculate the PV output power P_{PV}, the following equation can be used [50]:

$$P_{PV} = P_{STC}\frac{I_S}{1000}\left[1 + \gamma(T_C - 25)\right] \quad (35)$$

Where, P_{STC} is the maximum power of the PV module under standard test conditions (STC) (W); I_S is the solar irradiation on the surface of the PV module (W/m^2); is the PV module temperature coefficient for power in (°C-1); T_C is the temperature of the PV cell (module) in (C). The temperature of PV module can be calculated based on solar irradiance and ambient temperature based on the Nominal Operating Cell Temperature (NOCT) of the module. The NOCT model equation is [50]-[51]:

$$T_c = T_a + \frac{I_S}{800}\left(T_{NOCT} - 20\right) \quad (36)$$

T_a and T_{NOCT} are the ambient temperature and the NOCT of the module in (°C).

3 Diesel generators (DEG)

Usually, diesel fuel consumption data in (L/h) at 25%, 50%, 70% and 100% of rated DEG power (kW) is provided by the manufacturer. Based on these data, the fuel consumption characteristic of the DEG can be estimated as a quadratic function of its active power output:

$$Fuel_{DEG} = a_f P_{DEG}^2 + b_f P_{DEG} + c_f \quad (37)$$

Where, $Fuel_{DEG}$ is the fuel consumption in (L/h); P_{DEG} is the DEG power output in (KW);

α_f, b_f and c_f are the coefficients of the fuel consumption characteristic. As a result, the DEG bids ($/h) can be calculated as:

$$B_G = C_{fuel} Fuel_{DEG} + C_{inv} \quad (38)$$

C_{fuel} is the price of diesel fuel to supply DEG in ($/L). C_{inv} is the hourly payback amount for the investment cost of the DEG ($/h) defined by (31).

4 Electric grid

Market energy costs ($/h) can be represented by a quadratic function as follows:

$$f_{gr} = a + bP_{gr} + cP_{gr}^2 \quad (39)$$

Where, f_{gr} is the electrical power of electrical network in (kW) and a, b and c are the cost coefficients. For example, in the OPF cases, the values of the coefficients were adopted as $a = 0$, b in ($/kW h) and c in ($/kW2 h) [41].

2.4. Input random variables

Wind speed and solar irradiation modelling requires a probability distribution because they are random (stochastic) phenomena phenomenon. To determine the wind speed and solar irradiation, various probability distributions were used, but the Weibull distribution compared to other distributions is the most widespread and recognized in the specific research in wind and solar energy.

1 Weibull distribution

The probability density function (PDF) of the wind speed at a certain location is, generally, described by a *Weibull distribution* [42], [48], [50]:

$$f_{P_{WT}}(P_{WT}) = \frac{k}{C}\left(\frac{P_{WT}}{C}\right)^{k-1} e^{(P_{WT}/C)^k} \quad (40)$$

The CDF of *Weibull distribution* is

$$F_{P_{WT}}(P_{WT}) = 1 - e^{-(P_{WT}/C)^k} \quad (41)$$

The CDF with its inverse is used to calculate the wind speed is

$$P_{WT} = C(-\ln(r))^{1/k} \quad (42)$$

Where, r are the random numbers uniformly distributed over [0, 1]. The constants *C* and *k* are the scale and shape parameters of the *Weibull distribution*. Generally, the parameters *C* and *k* are calculated, approximately, using the Wind speed average v_m and standard deviation (SD) σ as follows [41]-[42]

$$\begin{cases} k = \left(\dfrac{\sigma}{P_{WTm}}\right)^{-1.086} \text{ and } \\ C = \dfrac{P_{WTm}}{\Gamma(1+1/k)} \end{cases} \quad (43)$$

Where, $\Gamma(x)$ is the gamma function defined as:

$$\Gamma(x) = \int_0^\infty t^{x-1} e^{-t}\, dt \quad \text{for} \quad x > 0 \quad (44)$$

2 Normal distribution

Basically, solar irradiation has a stochastic nature. The uncertainty of solar irradiation can be characterized by a normal probability density function [50].

$$f_{IS}(I_S) = \frac{1}{\sigma\sqrt{2\pi}} e^{-(I_S-\mu)^2/2\sigma^2} \quad (45)$$

The CDF for the normal distribution is:

$$F_{IS}(I_S) = \frac{1}{2}\left[1 + erf\left(\frac{(I_S-\mu)}{\sqrt{2\sigma}}\right)\right] \quad (46)$$

The CDF with its inverse was used to calculate the solar irradiation

$$I_S = \mu + \sqrt{2}.\sigma.erf^{-1}(2r-1) \quad (47)$$

Where, r is a random variable with uniform distribution in [0, 1]; μ is the mean value of I_S, and σ is the SD of I_S; erf and erf^{-1} are the error and the inverse error functions, respectively, defined as follows

$$\begin{cases} erf(I_S) = \dfrac{2}{\sqrt{\pi}} \displaystyle\int_0^{I_S} e^{-t^2} dt \\ erf^{-1}(I_S) = 1 - erf(I_S) = \dfrac{2}{\sqrt{\pi}} \displaystyle\int_{I_S}^{\infty} e^{-t^2} dt \end{cases} \quad (48)$$

The morning period, afternoon period, and hours around the solar noon, can be used for determined the SD of the hourly average value of the solar irradiation [41], [50]. At the end of the simulation test, it was assumed that the hourly averages of solar irradiation, μ are equal to their predicted values (forecasted), and the values of σ are predetermined with $(\sigma/\mu).100 = 8\%$ at

morning (from 5–8h) and evening hours (from 17–21h), and 3% around solar noon (9–16h).

3 Probabilistic load modelling

The load can be assumed to be a random variable (L) following the same PDF every hour of a given daily load diagram. It is assumed that the PDF of the active/reactive power load is under lower than the normal distribution [50]:

$$f_L(L)=\frac{1}{\sigma\sqrt{2\pi}}e^{-(L-\mu)^2/2\sigma^2} \quad (49)$$

Where, μ is the mean value shown as the fixed load level on the daily load diagram (DLD); σ is the SD of L. The normal CDF (49) with its inverse (51) was used to generate the load value

$$F_L(L)=\frac{1}{2}\left[1+erf\left(\frac{(L-\mu)}{\sqrt{2\sigma}}\right)\right] \quad (50)$$

$$L=\mu+\sqrt{2}.\sigma.erf^{-1}(2r-1) \quad (51)$$

Where, r is a random variable having a uniform distribution at [0, 1]; erf and erf^{-1} are defined in (48).

3. PARTICLE SWARM OPTIMIZATION

PSO is a new optimization method developed by Kennedy and Eberhart [52]. This algorithm is designed on the basis of social behavior processes associated with a flock of birds; essentially it is one of evolutionary computation techniques. It uses a number of particles that constitute a swarm. Each particle traverses the search space looking for the global minimum (or maximum). In a PSO system, particles fly around in a multidimensional search space. During flight, adjustment of position for both particles is reached according to its own experience, and neighboring particles experience, taking use of the best position encountered by itself and its neighbors. The swarm direction of a particle is defined by the set of particles neighboring, the particle and its history experience [5], [53]. The best previous position of a particle is recorded and represented as $pbest$. The position of the best particle among all the particles is represented as $gbest$. For each particle, the velocity and position can be calculated using [5], [54]

$$v_j^{(i+1)}=k\left[\begin{array}{l} w.v_j^{(i)}+c_1 rand_1.(pbest_j-x_j^{(i)}) \\ \quad +c_2 rand_2.(gbest_j-x_j^{(i)}) \end{array}\right] \quad (52)$$

$$x_j^{(i+1)}=x_j^{(i)}+v_j^{(i+1)} \quad \forall\ j=1,2,3,.....n_S \quad (53)$$

Where x_j and v_j are, respectively, the current position and particle velocity of at the j^{th} generation, w is the factor of inertia weight. c_1 and c_2 are the acceleration constants, n_S is the number of the swarms, and $rand$ are random numbers between 0 and 1. Generally, w can be expressed by [14], [39] [53]-[55]:

$$w=w_{\max}-\frac{w_{\max}-w_{\min}}{i_{\max}}.i \quad (54)$$

Where, $i_{\max}$ is the maximum number of iterations, i is the current iterations. $w_{\max}$ and $w_{\min}$ are the high and lower limits of inertia weight it decreases linearly in each run from 0.9 to 0.4. k is a factor constriction derived from the stability analysis of equation (52) to ensure the system to converge but not prematurely. Mathematically, k can be expressed by

$$k=\frac{2}{\left|2-c-\sqrt{c^2-4c}\right|} \quad (55)$$

where $c=c_1+c_2$ and $c>4$

The particle velocity is limited by a maximum value $V_{\max}$ .Based on the experiences with the PSO methods, $V_{\max}$ is often set at 10% to 20% of the dynamic range of the variable on each dimension [14], [54]-[57].

4. RESULTS AND DISCUSSION

The MG (Fig. 1) is used in this work. The MG is considered in order to show how to determine the offers of the different DG units. The system is a MG composed of five different DG units (WT connected to bus 4, a MT is connected to bus 7, a PV connected to bus 11, a DEG connected to bus 19 and an FC connected to bus 23) with SSEs and electrical loads. Table 1 presents the data was used to calculate the DG bids coefficients and power limits of DG units. The 24-hour load demand profile and forecast energy market prices are shown in Table 2. It is assumed that all DG sources produce

active power at a single power factor. Based on the decisions of the MG Central Controller (MGCC), there is a power exchange link for one day between the utility and MG.

The PSO method is implemented to find optimal solutions of the GEO and OEM problems of the MG in an operating scenario as follows: It is assumed that the PV and WT sources act at their maximum power available during each hour of the day, and the other DGs, including MT, FC and DEG, can operate within their power limits while satisfying the necessary constraints.

All DGs with relevant characteristics generate electricity in the MG, and the additional demand or surplus energy inside the grid is exchanged with the utility from the point of common coupling PCC. The utility behaves as an unconstrained unit and exchanges power with the MG without any limitations.

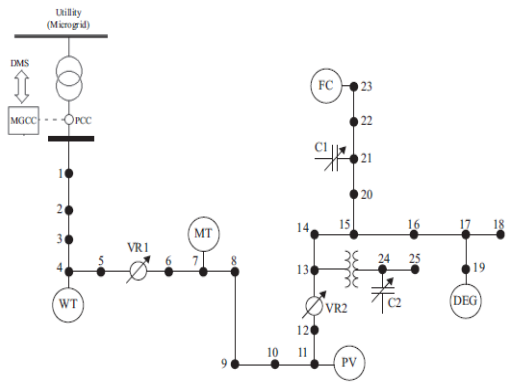


Fig. 1 One line diagram of test system.

Table 1 Power limits and bid coefficients of DG.

N° bus	Type	P_{DG}^{min} (KW)	P_{DG}^{max} (KW)	Cost coefficients		
				a	*B*	*c*
23	*FC*	30	300	0.006	1.62	2.204
19	DEG	0	369	0.006	12.41	1.177
11	PV	0	250	0	43.57	0
7	MT	90	300	0.002	2.63	811
4	WT	0	600	0	6.5	0
0	Utility	0	300	0	1e-8	5e-7

In this scenario, the influence of exchanges of energy market price with the utilities on the total operating cost of the MG is examined in the following 3 cases:

Case 1: Energy market price is low;

Case 2: Energy market price is average;

Case 3: Energy market price reaches its real value.

It was assumed that the active and reactive power of the load on each bas varies according to the daily load diagram shown in figure 2 compared to the nominal values. Graphical data's of wind speed, ambient temperature, solar irradiance and energy market price are shown in figures 3-6, respectively, both figures are scaled for 24 h.

Given the low market price in the 1st case, especially during periods when the load levels are low and medium, the utility takes the lead in supplying the load inside the MG.

In the 2nd case, when the market price is middle range (higher compared to case 1), most of the load portion is provided by MT and FC units. During periods of average load, corresponding to the average market price (5.6 $/kWh), excess energy is exported from the MG to the utility.

Table 2 Forecast load and market prices.

Time [h]	Load [MW]	Market prices ($/kWh)		
		Case 1	Case 2	Case 3
1	480	1.4	2.8	3.5
2	480	1.4	2.8	3.5
3	600	1.4	2.8	3.5
4	600	1.4	2.8	3.5
5	720	2.8	5.6	7
6	720	2.8	5.6	7
7	840	2.8	5.6	7
8	840	2.8	5.6	7
9	960	2.8	5.6	7
10	960	2.8	5.6	7
11	1080	4.2	11.2	12.6
12	1080	4.2	11.2	12.6
13	1200	4.2	11.2	12.6
14	1200	4.2	11.2	12.6
15	1080	4.2	11.2	12.6
16	840	2.8	5.6	7
17	840	2.8	5.6	7
18	960	2.8	5.6	7
19	1080	4.2	11.2	12.6
20	1080	4.2	11.2	12.6
21	960	2.8	5.6	7
22	840	2.8	5.6	7
23	720	2.8	5.6	7
24	600	1.4	2.8	3.5

When the market price is brought to its real value in the 3rd case, the MT and FC units are used with their maximum power in periods with medium and high loads levels. In addition, surplus energy is exported from the MG to the utility in most period of the day. The simulation results associated with cases 1, 2 and 3 are shown in figures 7-14, respectively.

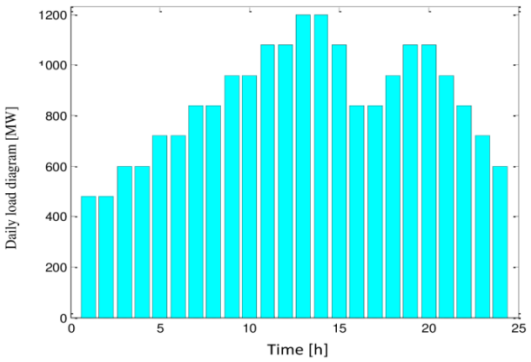


Fig. 2 Daily load diagram data.

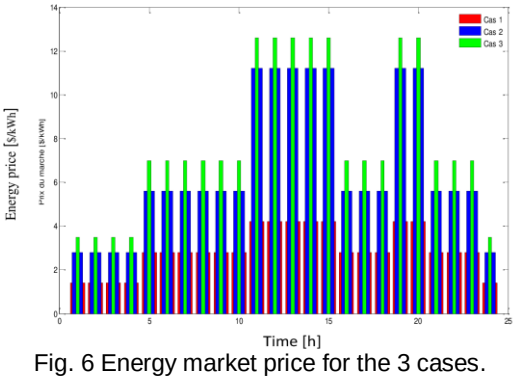


Fig. 6 Energy market price for the 3 cases.

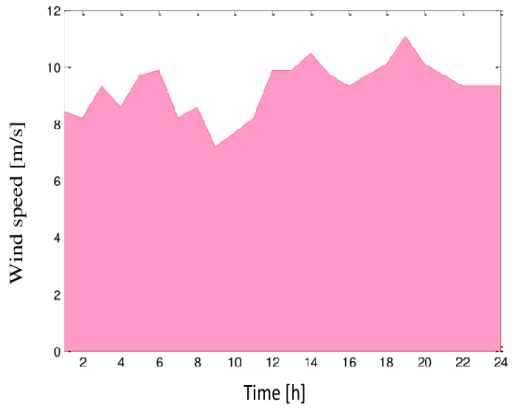


Fig. 3 Wind speed data.

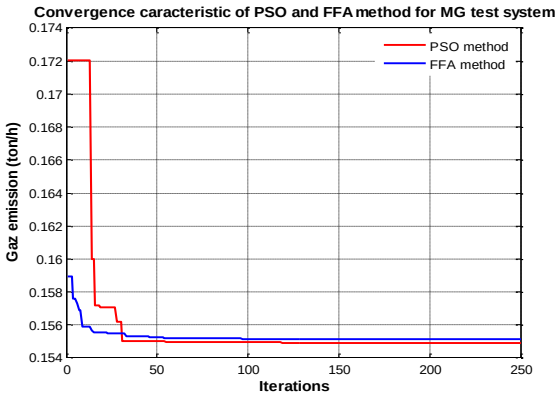


Fig. 7 Gas emission optimization.

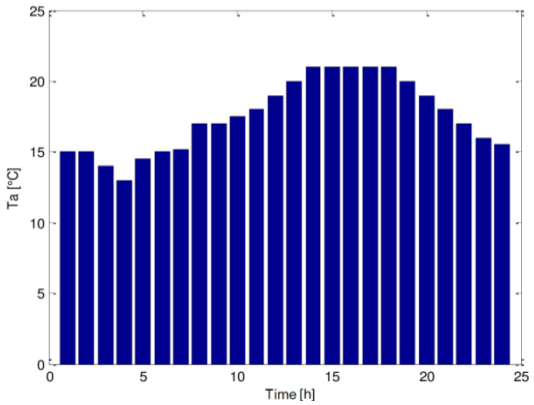


Fig. 4 Ambient temperature data.

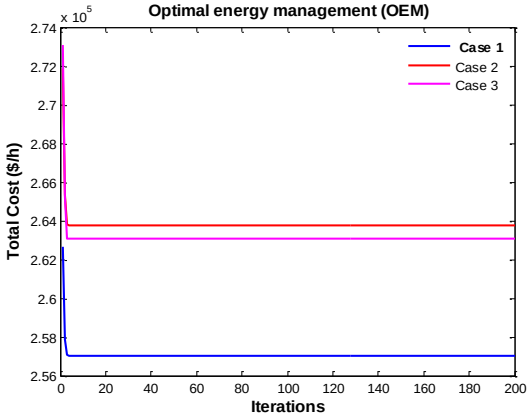


Fig. 8 Costs for the 3 cases.

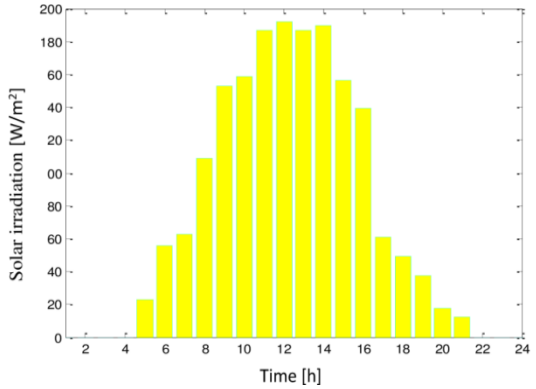


Fig. 5 Solar irradiation data.

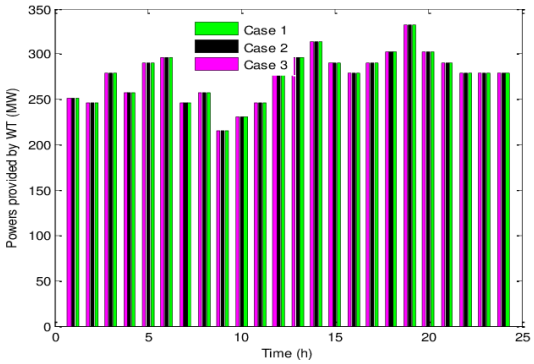


Fig. 9 Powers provided by the WT.

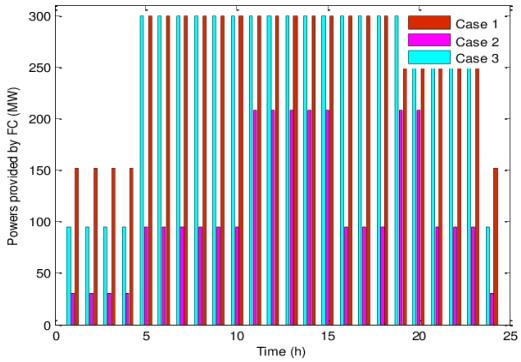


Fig. 10 Powers provided by the FC.

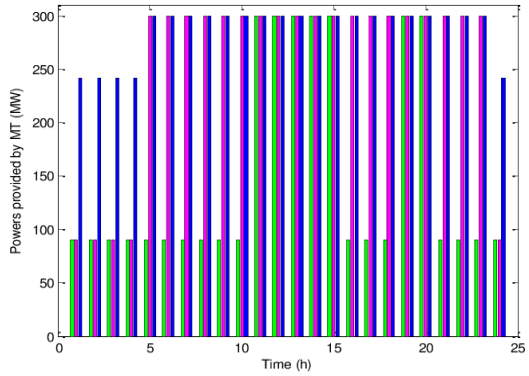


Fig. 11 Powers provided by the MT.

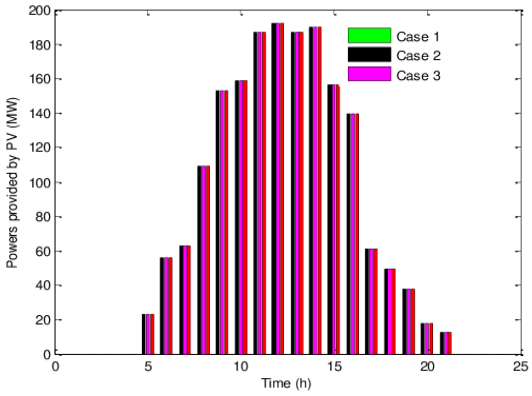


Fig. 12 Powers provided by PV moduls.

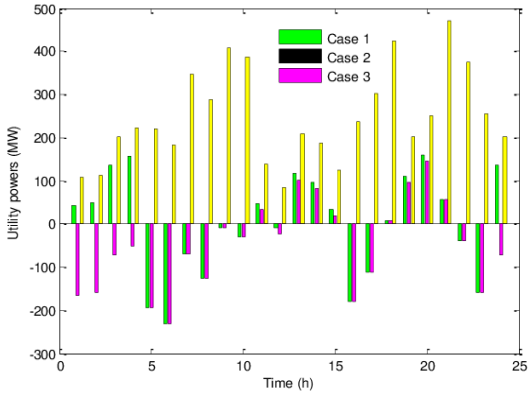


Fig. 13 Utility powers.

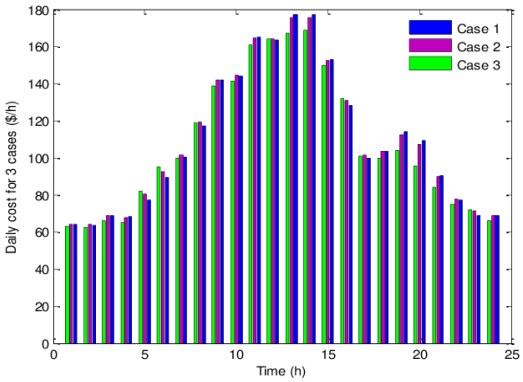


Fig. 14 Daily costs of 3 cases.

Table 3 Active and reactive power generations.

DGs	Optimal values			
	PSO		FFA	
	P [MW]	Q [MVAr]	P [MW]	Q [MVAr]
WT	230.4	111.6	230.4	111.6
MT	300.0	145.3	300.0	145.3
PV	158.8	76.9	158.8	76.9
DEG	140.4	68.0	143.2	69.3
FC	300.0	-200.0	300.0	225.0
Utility	385.7	376.1	368.8	-22

Table 4 Control variable of case 1.

Control variables	Methods	
	PSO	FFA
PG_7 (MW)	0.3000	0.3000
PG_{19} (MW)	0.1404	0.1432
PG_23 (MW)	0.3000	0.3000
PG_{11} (MW)	0.1588	0.1588
PG_4 (MW)	0.2304	0.2304
V_0 (pu)	1.0499	1.0148
V_{23} (pu)	0.9800	1.0499
Qcom21 (MVAr)	0.3000	0.2073
Qcom24 (MVAr)	0	0.0644
$T_{5\text{-}6}$	0.9786	0.9627
$T_{12\text{-}13}$	0.9667	0.9652
Cost in ($/h)	143.958	142.03
Losses (MW)	6.30	4.82
GEO (ton/h)	0.154	0.155
CPU time (s)	205.184	177.133

5. CONCLUSION

An effective approaches based on PSO method is successfully applied to solve the GEO and OEM problems of a MG. *Weibull* and *normal distributions* are used to model the input variables, namely the PV and WT output powers, the load demand and the market price. The proposed PSO has been tested and studied on a MG comprising different DG units with an ESS. The simulation results show the effectiveness of proposed approach to solve the GEO and OEM problems in different operational scenarios. Moreover, the obtained results using PSO are either better or comparable to

those obtained by other in the literature. In terms of the computational effort, convergence speed and performance of solutions reveal the superiority of PSO algorithm.

References

[1] M. F. Zia, et al., ‘‘Energy management system for an islanded microgrid with convex relaxation’, IEEE Transactions on Industry Applications, vol. 55, no.6, pp. 7175–7185, 2019.

[2] H. Wu, H. Li, and X. Gu, ‘‘Optimal energy management for microgrids considering uncertainties in renewable energy generation and load demand’, Processes, vol. 8, no. 9, p. 1086, 2020.

[3] Talaq, J. H., El-Hawary, F. and M. E. El-Hawary. “A Summary of Environmental/economic Dispatch Algorithms“, IEEE Transactions on Power Systems. 9, no. 3, pp. 1508–1516, 1994.

[4] Mohamed, A. A. A., El-Gaafary, A. A. M., Mohamed, Y. S. and Hemeida, A. M. “Multi-Objective Modified Grey Wolf Optimizer for OPF“, IEEE Eighteenth International Middle East Power Systems Conference. 27-29/12/2016.

[5] Kumar, C. and Raju, Ch. P. “Constrained OPF using Particle Swarm Optimization. Int. J. of Em. Tech. and Adv. Eng. Vol. 2, no. 2, pp. 235–241, 2012.

[6] H. Jiayi, J. Chuanwen, and X. Rong, ‘‘A review on distributed energy resources and microgrid’’, Renewable and Sustainable Energy Reviews, vol. 12, pp. 2472–2483, 2008.

[7] F. A. Mohamed, and H. N. Koivo, “Online management genetic algorithms of microgrid for residential application’, Energy Conversion and Management, vol. 64, pp. 562–568, 2012.

[8] C. Chen, et al., “Smart energy management system for optimal microgrid economic operation“, IET renewable power generation, vol. 5, no. 3, pp. 258–267, 2011.

[9] J. Radosavljevic´, M. Jevtic´, and D. Klimenta, “Energy and Operation Management of a microgrid using particle swarm Optimization’, Engineering Optimization, vol. 48, No. 5, pp. 811–830, 2016.

[10] J. A. P. Lopes, C. L. Moreira, and A. G. Madureira, “Defining control strategies for microgrids islanded operation’, IEEE Transactions on power systems, vol. 21 no. 2, pp. 916–924, 2006.

[11] N. D. Hatziargyriou, et al., “Quantification of economic, environmental and operational benefits due to significant penetration of microgrids in a typical LV and MV Greek network“, European Transaction on Electrical Power, vol. 21, no. 2, pp. 1217–1237, 2011.

[12] A. G. Tsikalakis, N. D. Hatziargyriou, “Centralized control for optimizing microgrids operation“, IEEE Transactions on Energy Conversion, vol. 23, No. 1, pp. 241–248, 2008.

[13] T. S. Ustun, C. Ozansoy, and A. Zayegh, “Recent developments in microgrids and example cases around the world—a review”, Renewable and Sustainable Energy Reviews, vol. 15, pp. 4030–4041, 2011.

[14] J. Radosavljević, et al, “Optimal power flow for distribution networks with distributed generation”, Serbian Journal of Electrical Engineering, vol. 12, no. 2, pp. 145–170, 2015.

[15] D. Tenfen, and E. C. Finardi, “A mixed integer linear programming model for the energy management problem of microgrids”, Electric Power Systems Research, vol. 122, pp. 19–28, 2015.

[16] A. Arabali, M. Ghofrani, M. E. Amoli, S. Fadali, and Y. Baghzouz, “Genetic-algorithm-based optimization approach for energy management”, IEEE Transactions on Power Delivery, vol. 28, No. 1, pp. 162–170, 2013.

[17] E. Kuznetsova, C. Ruiz, Y. F. Li, and E. Zio, “Analysis of robust optimization for decentralized microgrid energy management under uncertainty”, International Journal of Electrical Power & Energy Systems, vol. 64, pp. 815–832, 2015.

[18] N. Nikmehr, and S. N. Ravadanegh, “Optimal operation of distributed generations in micro-grids under uncertainties in load and renewable power generation using heuristic algorithm”, IET Renewable Power Generation, vol. 9, no. 8, pp. 982–890, 2015.

[19] F. A Mohamed, and H. N. Koivo, “System modelling and online optimal management of microgrid using mesh adaptive direct search’, International Journal of Electrical Power & Energy Systems, vol. 32, no. 5, pp. 398–407, 2010.

[20] P. Li, W. Xu, Z. Zhou, and R. Li, “Optimized operation of microgrid based on gravitational search algorithm”, Proceedings of International Conference on Electrical Machines and Systems, Busan, Korea, pp. 338–42, 2013.

[21] M. A. Ríos and M. A. V. Rodríguez, “Multi-objective Firefly Algorithm for Energy Optimization in Grid Environments”, International Conference on Swarm Intelligence, LNTCS, vol. 7461, pp 350–351.

[22] W. A. Hasan, I. A. Abed, D. K. Shary, “Energy Management Optimization of Generators Using Modified Firefly Algorithm”, 2nd International Multi-Disciplinary Conference Theme: Integrated Sciences and Technologies, IMDC-IST, 7–9, Sakarya, Turkey, September 2021.

[23] M. A. Kamarposhti, I. Colak, and K. Eguchi, “Optimal energy management of distributed generation in micro-grids using artificial bee colony algorithm”, Mathematical Biosciences and Engineering, vol. 18, no. 6, pp. 7402–7418, 2021.

[24] B. H. Ocaña, et al., “Bacterial Foraging-Based Algorithm for Optimizing the Power Generation of an Isolated Microgrid”, Applied Sciences, vol. 9, no. 6, pp.1261, 2019.

[25] M. Y. Alsmadi, et al., “Optimal configuration and energy management scheme of an isolated micro-grid using Cuckoo search optimization algorithm”, Journal of the Franklin Institute, vol. 356, no., pp. 4191–4214, May 2019.

[26] N. M. Isa, T. C. Wei, A. H. M. Yatim, "Energy Management for an Islanded Microgrid Based on Harmony Search Algorithm", 41st International Spring Seminar on Electronics Technology (ISSE), pp. 16–20 May 2018.

[27] K. F. Fong, V. I. Hanby, T. T. Chow, "HVAC system optimization for energy management by evolutionary programming", Energy and Buildings, vol. 18, no. 3 pp. 220–231, March 2006.

[28] S. Mandal, K. Mandal, "Optimal energy management of microgrids under environmental constraints using chaos enhanced differential evolution", Renewable Energy Focus, vol. 34, pp. 129–141, September 2020.

[29] B. Bentouati et al., "An enhanced moth-swarm algorithm for efficient energy management based multi dimensions OPF problem", Journal of Ambient Intelligence and Humanized Computing, vol. 12, no. 1, pp. 1–21, 2020.

[30] N. Javaid, et al., "A Hybrid Genetic Wind Driven Heuristic Optimization Algorithm for Demand Side Management in Smart Grid, Energies, vol. 10, no. 3, pp. 319–346, 2017.

[31] R. Krishna and S. Hemamalini, "Optimal Energy Management of Virtual Power Plants with Storage Devices Using Teaching-and-Learning-Based Optimization Algorithm", International Transactions on Electrical Energy Systems, vol. 2022, pp. 1–17, 2022.

[32] I. Hussain et al., "Smart Energy Management System for University Campus using Sine-Cosine Optimization Algorithm", International Virtual Conference on Power Engineering Computing and Control: Developments in Electric Vehicles and Energy Sector for Sustainable Future (PECCON), 05-06 May 2022.

[33] A. R., M. Sadeghi, J. Agha, "Modified imperialist competitive algorithm for environmental constrained energy management of microgrids", Journal of Cleaner Production, vol. 20, pp. 273-292, 2018.

[34] J. D. Tan, et al., "An Electromagnetism-like Mechanism Algorithm Approach for Photovoltaic System Optimization", Indonesian Journal of Electrical Engineering and Computer Science, vol. 12, no. 1, pp. 333–340.

[35] A. Esmat, et al., "A novel Energy Management System using Ant Colony Optimization for micro-grids", 3rd International Conference on Electric Power and Energy Conversion Systems (EPECS), 2013.

[36] S. Debata, C. K. Samanta, and S. P. Panigrahi, "Efficient energy management strategies for hybrid electric vehicles using shuffled frog-leaping algorithm", International Journal of Sustainable Engineering, vol. 8, No. 2, pp. 1–7, 2015.

[37] K. Sabah, et al., "Grey Wolf Optimization-Based Optimum Energy-Management and Battery-Sizing Method for Grid-Connected Microgrids", Energies, vol. 11, no. 4, pp. 847-864, 2022.

[38] N. Mezhoud, B. Ayachi, M. Amarouayache, "Multi-objective optimal power flow based gray wolf optimization method", Electrical Engineering and Electromechanics,, vol. 22, no. 4, pp. 57–62, 2022.

[39] Mezhoud, N., Leulmi, S. and Boukadoum. "AC-DC OPF Incorporating Shunt FACTS Devices using HVDC Model and Particle Swarm Optimization Method". International Review of Electrical Engineering (IREE), vol. 2, 382-393, 2014.

[40] Nabil Mezhoud, "Multi-objective Optimal Power Flow and Emission Index Based Firefly Algorithm".Periodica Polytechnica Electrical Engineering and Computer Science, vol. 67, no. 2, pp. 172–180, 2023.

[41] J. Radosavljević, "Metaheuristic Optimization in Power Engineering", The Institution of Engineering and Technology, Michael Faraday House, Six Hills Way, Stevenage, Herts, SG1 2AY, United Kingdom, 2018.

[42] Y. Zhang, N. Gatsis, and G. B. Giannakis, "Robust energy management for microgrids with high-penetration renewable", IEEE Transactions on Sustainable Energy, vol. 4, no. 4, pp. 944–953, 2013.

[43] Wu H., Liu X., Ding M. "Dynamic economic dispatch of a microgrid: Mathematical Models and Solution Algorithm", International Journal of Electrical Power and Energy Systems, vol. 63, pp. 336–346, 2014.

[44] A. A. Moghaddam, A. Seifi, T. Niknam, and M. R. A. Pahlavani, "Multi-objective operation management of a renewable MG (micro-grid) with back-up micro-turbine/fuel cell/battery hybrid power source", Energy, vol. 36, pp. 6490–6507, 2011.

[45] A. M Azmy, I. Erlich, "Online optimal management of PEM fuel cells using neural networks". IEEE Transactions on Power Delivery, vol. 20, no. 2, pp 1051–1058, 2005.

[46] S. Campanari, and E. Macchi, "Technical and tariff scenarios effect on microturbine trigenerative applications", Journal of Engineering for Gas Turbines and Power, vol. 126, pp. 581-589, 2004.

[47] F. Barbir, and T. Gomez, "Efficiency and economics of proton exchange membrane (PEM) fuel cells". International Journal of Hydrogen Energy, vol. 22, no. 10/11, pp. 1027–1037, 1997.

[48] D. Villanueva, J. L. Pazos, and A. Feijo, "Probabilistic load flow including wind power generation". IEEE Transactions on Power Systems, vol. 26, no. 3, pp. 1659–1667, 2011.

[49] Y. M Atwa., E. F. El-Saadany, M. M. M. Salama, R. Seethapathy, M. Assam, and S. Conti, "Adequacy evaluation of distribution system including wind/solar DG during different modes of operation", IEEE Transactions on Power Systems, vol. 26, no. 4, pp. 1945–52, 2011.

[50] W. B. Wan Nika, M. Z. Ibrahimb, K. B Samoa, and A. M. Muzathika, "Monthly mean hourly global solar radiation estimation", Solar Energy, vol. 2012, pp. 86, pp. 379–387, 2012.

[51] G. N. Tiwari, and S. Dubey, "Fundamentals of photovoltaic modules and their applications", London: RSC Energy Series Cambridge, pp. 423. 2010.

[52] Kennedy, J. and Eberhart, R. "Particle Swarm Optimization ". Proceedings of the IEEE International Conference on Neural Networks, 4: pp. 1942–1948, 1995.

[53] Hazra, J. and Sinha, A. K. “A Multi-objective Optimal Power Flow using Particle Swarm Optimization“. Euro. Trans. Electr. Power, vol. 21, no. 1, pp. 1028-1045, 2010.

[54] C. Kumar and Ch. Padmanabha Raju, "Constrained Optimal Power Flow using Particle Swarm Optimization", International Journal of Emerging Technology and Advanced Engineering, vol. 2, no. 2, 2012.

[55] Jong Yul Kim, Hwa-Seok Lee and June Ho Park, "A Modified Particle Swarm Optimization for Optimal Power Flow", Journal of Electrical Engineering and Technology, vol. 2, no. 4, pp. 413–419, 2007.

[56] Davoud Sedighizadeh and Ellips Masehian, "Particle Swarm Optimization Methods, Taxonomy and Application", International Journal of Computer Theory and Engineering, vol. 1, no. 5, pp. 1793–8201, December 2009.

[57] Barzegari, A., Barforoushi, T., Asgharpour, H., Lesan, S., "A new algorithm based on particle swarm optimization for solving power economic dispatch considering valve-point effects and emission constraints", International Review on Modelling and Simulations (IREMOS), vol. 4, no. 3, pp. 1303–1311, 2011.